

Influence of pinning states on dynamic phase transitions in a driven vortex lattice

This article has been downloaded from IOPscience. Please scroll down to see the full text article.

2002 J. Phys.: Condens. Matter 14 5391

(<http://iopscience.iop.org/0953-8984/14/21/313>)

View [the table of contents for this issue](#), or go to the [journal homepage](#) for more

Download details:

IP Address: 171.66.16.104

The article was downloaded on 18/05/2010 at 06:44

Please note that [terms and conditions apply](#).

Influence of pinning states on dynamic phase transitions in a driven vortex lattice

V G Prokhorov¹ and Y P Lee^{2,3}

¹ Institute of Metal Physics, National Academy of Sciences of Ukraine, Kiev, 03142, Ukraine

² Department of Physics, Hanyang University, Seoul, 133-791, Korea

E-mail: yplee@hanyang.ac.kr

Received 12 October 2001, in final form 13 March 2002

Published 16 May 2002

Online at stacks.iop.org/JPhysCM/14/5391

Abstract

We have investigated the effect of an applied current on the vortex dynamics in superconducting amorphous Nb₃Ge and crystalline Pb₇₈Bi₂₂ thin films. We have observed a major difference between the scenarios for the vortex dynamic phase transition at high currents for the samples studied. In the amorphous Nb₃Ge films the transition of the flux line lattice from a pinning state to a moving coherent state occurs without an intermediate plastically deformed phase. In the Pb₇₈Bi₂₂ films the initial motion exhibits the characteristics of plastic (or incoherent) flow, which is ended by a sharp transition into the ordered state. We compare our data with the recent theories of ordering and phase transition in the moving vortex lattice.

Recently the dynamical behaviour of a flux line lattice (FLL) in type-II superconductors with different pinning states has attracted much attention [1, 2]. The unusual dynamics of the FLL originates from a competition between the vortex–defect and vortex–vortex interactions, leading to a phase transition in a driven FLL. If the pinning potential dominates, then the vortices are essentially stationary with a slow residual motion due to flux creep or tunnelling. In the opposite limit, when the pinning forces are weak compared with the driving force, the FLL is only elastically deformed and flows coherently. In the important intermediate regime, where the pinning and driving force are comparable, the FLL deforms plastically and an incoherent motion occurs. An actual dynamic phase transition between the plastically deformed phase and a moving ordered FLL was first proposed and numerically demonstrated in the two-dimensional (2D) approximation by Koshelev and Vinokur [3, 4]. It was shown that an increase in the FLL velocity leads to a diminution of the vortex–defect interaction and a moving defect-free crystal-like FLL phase is induced. To describe the transition, the concept of the ‘shaking temperature’ has been introduced, which measures the effective Langevin force

³ Author to whom any correspondence should be addressed.

exerted by the pinning centres on the moving vortices [4]. A more complicated dynamic phase diagram for driven FLL was recently predicted by Olson *et al* [5]. Two distinct dynamic phases of flux flow appear, depending on the vortex–vortex interaction strength. When the FLL is soft, the vortices flow in independently moving channels with a smectic structure. For the stiff FLL, adjacent channels become locked together, producing a crystal-like order in a coupled-channel phase. At the crossover the system produces the maximum amount of voltage noise, indicating that experimental voltage measurements can probe the FLL order.

Experimentally, a dynamical transition into a moving lattice phase has been suggested by transport measurements [6, 7], the neutron diffraction on flux lines in 2H-NbSe₂ [8], and the current–voltage characteristics for a 2D amorphous superconductor Mo₇₇Ge₂₃ [9]. The possibility of a current-induced increase in the spatial order of the vortex state has also been invoked to explain experimental results in superconducting/insulating multilayers of Mo₇₉Ge₂₁/Ge [10]. The nature of this current-induced ordering and its dependence on the pinning strength are, however, still in question.

In this paper, we present an investigation of the vortex dynamics in 2D thin films of amorphous Nb₃Ge and polycrystalline Pb₇₈Bi₂₂. We have observed a major difference between the mechanisms of the FLL dynamic phase transition at high currents for the samples studied. In the amorphous Nb₃Ge film the transition of the FLL from the pinning state to the moving coherent state (when the flux-flow resistance becomes independent of the current) occurs without an intermediate plastically deformed or ‘melted’ phase. In the Pb₇₈Bi₂₂ film we find that the onset of vortex motion occurs very abruptly as the current is increased, and that the initial motion exhibits characteristics of a plastic (or incoherent) flow, which is ended by a sharp transition into the ordered state. A dynamic phase diagram for the driven FLL for the Pb₇₈Bi₂₂ film is also proposed.

The experiments were performed on amorphous Nb₃Ge and polycrystalline Pb₇₈Bi₂₂ thin films prepared by electron-beam and thermal evaporation, respectively, as described elsewhere [11, 12]. For the Nb₃Ge films the superconducting transition temperature was $T_c = 3.2\text{--}3.8$ K, the residual resistivity was $\rho_0 = 160\text{--}190 \mu\Omega \text{ cm}$, and $dH_{c2}/dT|_{T_c} = 17\text{--}19 \text{ kOe K}^{-1}$, where H_{c2} is the upper magnetic critical field. The amorphous Nb₃Ge films belong to the group of dirty type-II superconductors, with London penetration depth $\lambda(0) \simeq 122$ nm and Ginzburg–Landau coherence length $\xi(0) \simeq 2.7$ nm ($\kappa \simeq 55$) in our case. For the Pb₇₈Bi₂₂ thin films $T_c = 7.5\text{--}8.3$ K, $\rho_0 = 6.1\text{--}8.4 \mu\Omega \text{ cm}$, and $dH_{c2}/dT|_{T_c} = 1.2\text{--}1.5 \text{ kOe K}^{-1}$. In contrast to the amorphous Nb₃Ge films, the Pb₇₈Bi₂₂ thin films can be treated as pure type-II superconductors, with $\lambda(0) \simeq 85$ nm and $\xi(0) \simeq 47$ nm ($\kappa \simeq 1.75$).

All the films investigated were homogeneous superconductors with low critical current density in zero external magnetic field, $j_c = 10^3\text{--}10^4 \text{ A cm}^{-2}$ for Nb₃Ge and $j_c = 10^4\text{--}10^5 \text{ A cm}^{-2}$ for Pb₇₈Bi₂₂. The pinning forces in these films are moderate and do not exceed $F_p \simeq 10^5\text{--}10^6 \text{ N m}^{-3}$.

The geometrical dimensions of samples were established by the photolithographic technique: the width was 0.325 mm, the distance between potential contacts was 3.65 mm, and the thickness d was between 100 and 200 nm. Using the superconducting parameter set and the expressions given in [13], we obtain the values for the Larkin correlation length of $600 \text{ nm} < L_c < 1.8 \mu\text{m}$ for the Nb₃Ge film and $1 \mu\text{m} < L_c < 4 \mu\text{m}$ for the Pb₇₈Bi₂₂ film. These values greatly exceed the thickness of samples and, from the point of view of the FLL, the films can be treated as 2D physical objects.

We employed the modulation technique to record the differential resistance of films as a function of the transport current (the first derivative of the current–voltage characteristics, dV/dI). The modulation current amplitude was selected within a range between 0.3 and 30 μA , which corresponds to $10^{-3}\text{--}10^{-1}$ of the maximum transport current. The highest

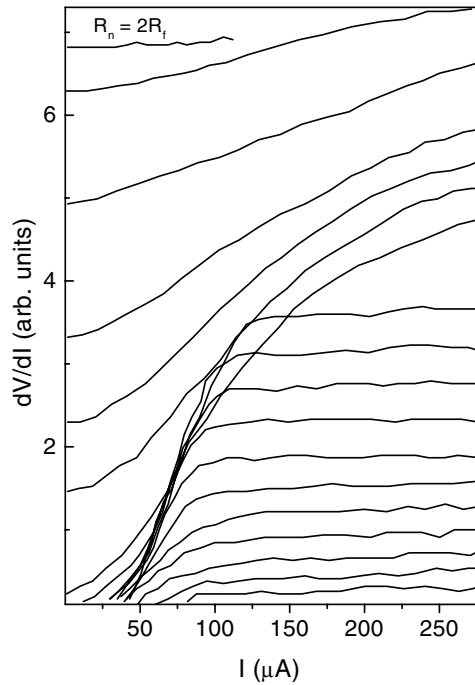


Figure 1. Differential resistance (dV/dI) versus current for an amorphous Nb_3Ge film at 2.83 K in different perpendicular applied magnetic fields (top to bottom): H (kOe) = 13.8, 8.1, 7.6, 7.0, 6.5, 6.2, 5.7, 4.5, 4.1, 3.8, 3.4, 2.9, 2.5, 2.1, 1.7, 1.3, 0.9, and 0.6. $R_n = 2R_f$ corresponds to Ohm's law at 13.8 kOe, which is displayed doubled. $d = 125$ nm and $T_c = 3.47$ K.

power dissipated in the samples did not go beyond 10 mW cm^{-2} even in a region where strong nonlinear effects were observed for dV/dI , which allowed us to exclude the influence of film overheating on the shape of experimental curves. All the experimental data were taken with the samples immersed in liquid ^4He and the measurements were carried out at temperatures below and at the λ -point for the superfluid helium transition to reduce Joule heating. The direction of applied magnetic field was always perpendicular to the film surface and the transport current.

Figure 1 shows a set of dV/dI versus I curves recorded for the amorphous Nb_3Ge film at different values of applied magnetic field. Two kinds of behaviour for dV/dI versus I can be distinguished on the experimental curves. At an external magnetic field of $B \leq 5.7$ kOe the classical flux-flow picture is observed: when the driving force exceeds the value of the vortex–pin interaction, the FLL undergoes a transition into a coherent flux-flow state. The magnetic field dependence of the flux-flow resistance (R_f), which is coincident with the current-independent value of the differential resistance in this case, exhibits a weak nonlinear behaviour and a good agreement with the Larkin–Ovchinnikov theory for superconductors with collective pinning [14] (see [15] for the more details). The inset of figure 2 presents the theoretical curves for R_f/R_n versus B , where R_n is resistance in the normal state, obtained using the values for upper magnetic critical field of $H_{c2} \simeq 15$ kOe ($T = 2.8$ K) and $\simeq 20$ kOe ($T = 2.5$ K) as a fitting parameter. The estimated values for H_{c2} practically coincide with experimental ones from $dH_{c2}/dT|_{T_c}$ at these temperatures.

It is worth noting that a decrease in temperature ($T \leq 2.2$ K) leads to the formation of a smooth and broad peak on the dV/dI versus I curves in a current range above the transition.

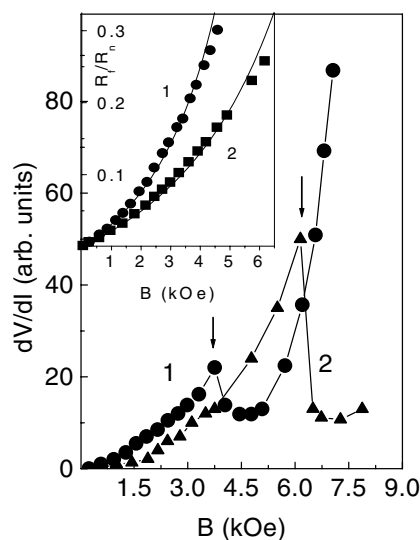


Figure 2. Differential resistance (dV/dI) as a function of magnetic field for an amorphous Nb_3Ge film at 2.5 K ('1') and 2.8 K ('2'). The modulation current amplitude and frequency were $30 \mu A$ and 1.96 kHz, respectively. Arrows indicate the onset of the peak effect. The curves are intended as a guide to the eyes. The inset shows the dependence of the normalized flux-flow resistance on magnetic field at 2.5 ('1') and 2.8 K ('2') for this sample.

A similar phenomenon was observed early on in the 2D amorphous $Mo_{77}Ge_{23}$ films [9] and interpreted as evidence for plastic and filamentary FLL flow. Unfortunately, this temperature range is lower than the λ -point of 4He , and the formation of a superfluid film on the surface of the sample can induce worse thermal conditions for the measurements.

If the applied magnetic field becomes larger than 5.7 kOe (see figure 1), the transition of the FLL into the flux-flow regime is accomplished not from the stationary pinning state, but from the excited resistive state, owing to the action of the ac measured current. If the superconductor demonstrates the 'peak effect' (a sharp increase of the critical current in a certain magnetic field region), then the minimum on the dV/dI versus B curve must occur with increasing external magnetic field. Figure 2 shows the resistive transition curves as a function of magnetic field for the amorphous Nb_3Ge film at two different temperatures and at a modulation current amplitude of $30 \mu A$ (a frequency of 1.96 kHz). Arrows indicate the onset of 'peak effect' for this film, which coincides with the previously obtained experimental data on the critical current and volume pinning force [16].

Figure 3 demonstrates a set of dV/dI versus I curves for the $Pb_{78}Bi_{22}$ film at various applied magnetic fields. In contrast to that for Nb_3Ge , the dependence exhibits a good distinct maximum which is ended by the transition of the FLL into the flux-flow regime. Consequently, the additional dynamic state of the driven FLL occurs between the disordered pinning and coherent flux-flow states in this film. This state produces a faster growth of voltage and its resistance is larger than the flux-flow one. This peculiarity smooths out and vanishes at smaller magnetic fields. At even higher currents, a deviation in dV/dI results from sample heating. The voltage rises sharply with decreasing magnetic field, and it is demonstrated that the nature of the resistive state is not connected with the motion of flux lines. On the contrary, the amplitude of the aforementioned peak depends directly on the magnetic field and reduces with decreasing field.

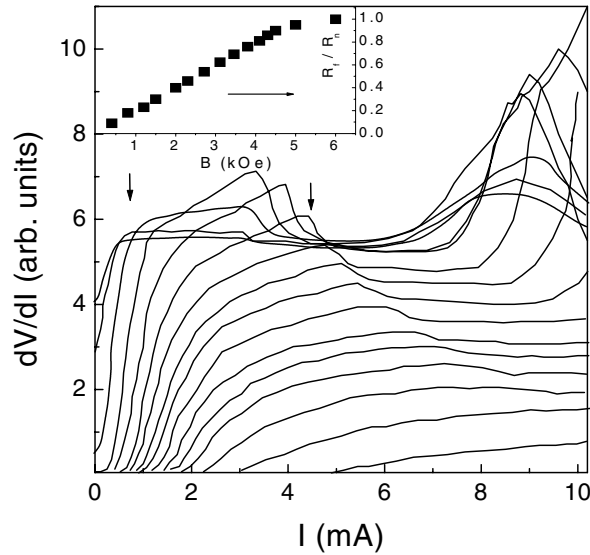


Figure 3. Differential resistance (dV/dI) versus current for a $\text{Pb}_{78}\text{Bi}_{22}$ film at 4.2 K in various perpendicular applied magnetic fields (left to right): H (kOe) = 5.35, 5.13, 4.95, 4.6, 4.26, 4.0, 3.65, 3.3, 2.95, 2.7, 2.35, 2.0, 1.82, 1.56, 1.22, and 0.52. The inset shows the dependence of the normalized flux-flow resistance on magnetic field at 4.2 K for this sample. $d = 155$ nm and $T_c = 8.3$ K.

The inset of figure 3 shows the dependence of the flux-flow resistance (R_f/R_n) on applied magnetic field. In contrast to that for the Nb_3Ge film (figure 2), this exhibits a linear behaviour in relation to magnetic field. The experimental data are precisely governed by the Bardeen–Stephen model [17] with $H_{c2} \simeq 6.5$ kOe as a fitting parameter. The estimated value is in good agreement with the magnitude obtained from $dH_{c2}/dT|_{T_c}$ for this sample.

Figure 4 shows the dynamic phase diagram for different states of the driven FLL with respect to applied magnetic field, based on figure 3 for the $\text{Pb}_{78}\text{Bi}_{22}$ film. Field A corresponds to the stationary pinned state of the lattice with a low voltage, which is generated mainly by a rearrangement of topological defects and a chaotic motion of the vortices. The phase boundary of this state is determined by the volume pinning force, $F_p = j_c B$. A range of an abrupt increase in voltage ($j \geq j_c$) is denoted by field B. At high magnetic field the B range has a quite distinct boundary with the plastically deformed driven FLL state (field C), which becomes smeared and vanishes with decreasing magnetic field. Range C is ended by a sharp drop in the differential resistance (see figure 3) and a transition of the FLL into a state with ordered and coherent flux flow (field D). It is worth noting that the boundary between fields C and D is also smeared when the applied magnetic field is decreased and that the aforementioned transition disappears at low magnetic fields. Therefore, the experimental results reveal clearly that there are three distinct dynamical phases in the $\text{Pb}_{78}\text{Bi}_{22}$ film, which were predicted theoretically [18].

The observed difference in dynamical behaviour of the FLL between the amorphous Nb_3Ge and the polycrystalline $\text{Pb}_{78}\text{Bi}_{22}$ films can be explained by the large difference in the pinning strength [13] ($j_c/j_0 \simeq 2.1 \times 10^{-6}$ for Nb_3Ge and 1.6×10^{-4} for $\text{Pb}_{78}\text{Bi}_{22}$, where j_0 is the depairing current density). It is quite possible that it is the much weaker pinning in the amorphous Nb_3Ge film that is responsible for the coherent FLL motion (outside of the ‘peak effect’ region), while the stronger pinning and the more disordered vortex lattice in the $\text{Pb}_{78}\text{Bi}_{22}$ film favour the formation of channels and plastic motion. Because the vortex–defect

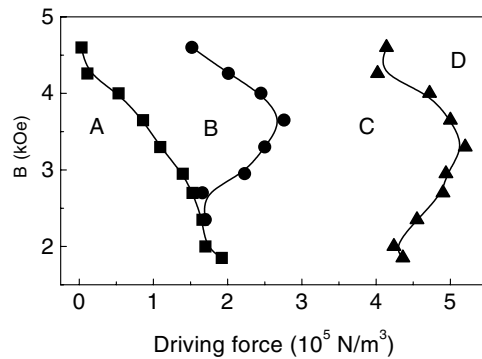


Figure 4. The dynamical phase diagram of the FLL states at various magnetic fields as a function of the driving force for a $\text{Pb}_{78}\text{Bi}_{22}$ film (figure 3) at 4.2 K. 'A' corresponds to the pinned state of the FLL, 'B' to the width of the transition from the pinned state to the plastically disordered state, 'C' to plastically disordered incoherent flow of the FLL, and 'D' to ordered coherent flow of the FLL.

interaction is larger than the vortex–vortex one in the $\text{Pb}_{78}\text{Bi}_{22}$ film (owing to the small κ and the high pinning strength), the plastic motion of the FLL turns out to be along the uncoupled flow channels at a certain driving force (field C in figure 4). In this regime of FLL motion, the first derivative of the current–voltage characteristics exhibits a well-defined linear behaviour (see figure 3). Consequently, the dependence of the electrical field on the transport current in this region can be described by a power law, $E \sim (1 - j/j_c)^2$. Note that a similar power law was predicted for the depinning activation energy of the plastically deformed driven FLL in the presence of a finite density of strong pinning centres [1]. Therefore, such V versus I behaviour can be explained by the combination of an increase in the number of vortex flow channels and an increased flow along each active channel as the current is increased. Because the increase in the driving force leads to a reduction of the effective pinning strength [4], the vortex–defect interaction becomes smaller than the vortex–vortex one at a certain applied current, and the adjacent channels become locked together, producing FLL flux flow in a coupled channel [5]. Therefore, the phase boundary between fields C and D in figure 4 defines the critical value for the driving force, which provides the dynamic phase transition of the FLL from the plastically disordered (incoherent flow) to the ordered (coherent flow) state.

The appearance of an extended current range with plastically deformed moving vortices in the $\text{Pb}_{78}\text{Bi}_{22}$ film is not so surprising. For example, such a phenomenon was already observed in the pure niobium superconductor which also has a small value of $\kappa \simeq 1$ [19]. However, in contrast with amorphous or multilayered films [9, 10], where the transition of the FLL to the plastically disordered state is accompanied by a 'peak effect' on the $j_c(B)$ curve, the $\text{Pb}_{78}\text{Bi}_{22}$ film exhibits the common behaviour of the critical current in relation to magnetic field without sharp growth near H_{c2} .

In conclusion, we have investigated the vortex dynamics of amorphous Nb_3Ge and polycrystalline $\text{Pb}_{78}\text{Bi}_{22}$ thin films. It was shown that in the amorphous Nb_3Ge films the transition of the FLL from the pinning state to the flux-flow regime occurs without an intermediate plastically deformed phase. The magnetic field dependence of the flux-flow resistance exhibits a weak nonlinear behaviour and can be described in the framework of the Larkin–Ovchinnikov theory for superconductors with collective pinning [14]. In the $\text{Pb}_{78}\text{Bi}_{22}$ films we found extended current ranges with plastically deformed motion of the FLL, which is ended by a sharp transition into the flux-flow regime. In contrast to that for the Nb_3Ge film,

the flux-flow resistance of $\text{Pb}_{78}\text{Bi}_{22}$ film reveals a linear behaviour in relation to magnetic field and is precisely governed by the Bardeen–Stephen model [17]. A dynamic phase diagram for the driven FLL for the $\text{Pb}_{78}\text{Bi}_{22}$ film is also proposed.

Acknowledgments

This work was supported by Korea Research Foundation grants (KRF-99-D00048 and KRF-2001-015-DS0015) and Hanyang University, Korea, given in the programme year of 2001, and by the Science and Technology Centre of Ukraine through Project no 1455.

References

- [1] Schönenberger A, Larkin A, Heeb E, Geshkenbein V and Blatter G 1996 *Phys. Rev. Lett.* **77** 4636
- [2] Ruck B J, Abele J C, Trodahl H J, Brown S A and Lynam P 1997 *Phys. Rev. Lett.* **78** 3378
- [3] Koshelev A E and Vinokur V M 1994 *Phys. Rev. Lett.* **73** 3580
- [4] Aranson I, Koshelev A and Vinokur V 1997 *Phys. Rev. B* **56** 5136
- [5] Olson S J, Reichhardt C and Nori F 1998 *Phys. Rev. Lett.* **81** 3757
- [6] Bhattacharya S and Higgins M J 1993 *Phys. Rev. Lett.* **70** 26
- [7] Marley A C, Higgins M J and Bhattacharya S 1995 *Phys. Rev. Lett.* **74** 3029
- [8] Yaron U 1995 *Nature* **376** 753
- [9] Hellerqvist M C, Ephron D, White W R, Beasley M R and Kapitulnik A 1996 *Phys. Rev. Lett.* **76** 4022
- [10] White W R, Kapitulnik A and Beasley M R 1994 *Phys. Rev. B* **50** 6303
- [11] Prokhorov V G, Kaminsky G G and Tret'yachenko C G 1986 *Low Temp. Phys.* **12** 684
- [12] Prokhorov V G, Kaminsky G G and Tret'yachenko C G 1990 *Physica B* **165+166** 1171
- [13] Blatter G, Feigel'man M V, Geshkenbein V B, Larkin A I and Vinokur V M 1994 *Rev. Mod. Phys.* **66** 1125
- [14] Larkin A I and Ovchinnikov Yu N 1986 *Nonequilibrium Superconductivity* (Amsterdam: North-Holland)
- [15] Prokhorov V G, Kaminsky G G and Tret'yachenko C G 1993 *Low Temp. Phys.* **19** 616
- [16] Prokhorov V G, Kaminsky G G and Tret'yachenko C G 1992 *Low Temp. Phys.* **17** 498
- [17] Bardeen J and Stephen M J 1965 *Phys. Rev. A* **140** A1197
- [18] Ryu S, Hellerqvist M C, Doniach S, Kapitulnik and Stroud D 1996 *Phys. Rev. Lett.* **77** 5114
- [19] Gammel P L *et al* 1998 *Phys. Rev. Lett.* **80** 833